Low-Temperature Phase Behavior of Vegetable Oil/Co-solvent Blends as Alternative Diesel Fuel

R.O. Dunn* and M.O. Bagby[1]

Oil Chemical Research, USDA, ARS, NCAUR, Peoria, Illinois 61604

ABSTRACT: Vegetable oils (triacylglycerols) have many characteristics that make them attractive candidates as renewable alternative fuels for compression-ignition (diesel) engines. Unfortunately, vegetable oils are too viscous to be compatible with modern direct-injection diesel fuel systems and engines. Co-solvent blending is a simple and flexible technology that reduces viscosity by mixing the oil with low molecular weight alcohol. A co-solvent (**A**), consisting of surfactant plus an amphiphilic compound, is added to solubilize otherwise nearly immiscible oil–alcohol mixtures into a single-layer (isotropic) solution. This work examines low-temperature phase behavior of two soybean oil (SBO)/methanol mixtures solubilized by **A** = unsaturated long-chain (C_{18}) fatty alcohol/medium-chain alkanol (*n*-butanol and 2-octanol), one SBO/methanol mixture solubilized by **A** = triethylammonium linoleate/2-octanol, and one SBO/95 wt% ethanol (E95) mixture solubilized by *n*-butanol. The E95-blend was further blended in 1:1 (vol/vol) mixtures with No. 2 diesel fuel. Two types of anisotropic phase behavior were observed; formation of a cloudy layer of solid crystals suspended in bulk solution (Type I) and formation of two immiscible liquid layers (Type II). The type of phase separation in a given solution was influenced by phase separation temperature (T_φ) relative to the crystallization characteristics of compounds in the SBO and fatty alcohol or amine constituents present in solution. Solutions with relatively low T_φ values experienced crystallization of small solid particles favoring Type I separations. Conversely, solutions with T_φ sufficient to avert crystallization of high melting point compounds favored Type II separations where T_φ = critical solution temperature ($T_{critical}$). Increasing the **A**/oil (SBO or No. 2 diesel/SBO mixture) mass ratio decreased T_φ while increasing the mass fraction of alcohol (methanol or E95) increased T_φ. This work shows that vegetable oil/**A**-based blends can be formulated with cold flow properties superior with respect to cloud point and comparable with respect to kinematic viscosity (ν) of methyl soyate (biodiesel), either neat or blended with petroleum middle distillates.

Paper no. J9269 in *JAOCS 77*, 1315–1323 (December 2000).

KEY WORDS: Alternative diesel fuels, anisotropic phase behavior, cloud point, co-solvency, kinematic viscosity, phase separation temperature.

Over the past two decades, interest in developing vegetable oil (triacylglycerol)-based alternative fuels for combustion in compression ignition (diesel) engines has steadily increased. During the early 1980s, engine tests showed that combustion of neat vegetable oils caused durability problems relating to incomplete combustion such as nozzle coking, engine deposits, ring sticking, and contamination of crankcase lubricant (1–5). These problems were traced to poor fuel atomization aggravated by relatively high kinematic viscosities (ν) of the vegetable oils (6). Subsequent emphasis was placed on developing conversion technologies to reduce ν.

Transesterification with alcohol to form monoalkyl fatty esters (biodiesel) has drawn much attention as a conversion technology. Soybean oil (SBO) fatty acid methyl esters (hereafter called methyl soyate) have many fuel properties including ν, specific gravity, cetane number, and gross heat of combustion that compare well with No. 2 diesel fuel. On the other hand, methyl esters have relatively poor low-temperature flow properties. For example, the cloud point (CP) of methyl soyate is 15–20°C higher than that of No. 2 diesel (7). Thus, only low-level (≤10 vol%) methyl soyate/No. 2 diesel blends will be tolerable during cold weather in moderate temperature climates. Furthermore, combustion of methyl esters in some cases slightly increases nitrogen oxides (NO_x) in exhaust emissions (8–11). Perhaps the most significant barrier is economics—methyl soyate typically costs 3–5 times more to produce (before taxes) than petroleum-based fuels.

Co-solvent blending is an another vegetable oil conversion technology with enormous potential. Such formulations typically consist of vegetable oil/short-chain alcohol (methanol or ethanol) mixtures solubilized by a co-solvent (**A**). Although vegetable oil/**A** blends are often referred to as "microemulsion" fuels, the frequency of cases where microemulsions are present is rare and limited to specific conditions (12,13). Mixtures of SBO and 95 wt% ethanol (E95) stabilized by *n*-butanol were reported to exhibit characteristics consistent with formation of microemulsions (14). Similar results were observed upon solubilization of a small concentration (≤1.5 wt%) of water in a triolein/2-octanol/methanol blend (15).

Blending with low-molecular weight alcohol reduces ν of vegetable oils by dilution. The **A**, which consists of one or more surfactant or amphiphilic compounds, is added for the purpose of solubilizing otherwise nearly immiscible vegetable

[1]Retired.

*To whom correspondence should be addressed at USDA, ARS, NCAUR, 1815 N. University St., Peoria, IL 61604-3999.

E-mail: dunnro@mail.ncaur. usda.gov

oil/alcohol mixtures (13,16). Secondary benefits of adding **A** include solubilization of additives to enhance cetane number, heats of combustion, and resistance to oxidation. Such blends typically have ν values comparable to fatty acid methyl esters and slightly higher than No. 2 diesel (17).

Although the American Society for Testing and Materials (ASTM) specification for diesel fuels [D975 (18)] requires a minimum cetane number of 40 for No. 2 diesel, SBO/**A**-based blends tend to have lower cetane numbers. Goering *et al.* (19) reported cetane numbers of 25.1 for SBO/*n*-butanol/E95 and 29.8 for SBO/(*n*-butanol/triethylammonium linoleate)/E95 blends. Adding primary alkyl nitrate improved cetane number; however, relatively massive quantities (~10 wt%) were necessary to meet the D975 standard. Nevertheless, audible engine knock during short-term (3.5 h) testing was no different for vegetable oil/**A**-based blends than the reference diesel fuel, indicating that ignition quality of such blends exceeds that predicted by low cetane numbers.

Vegetable oil/**A**-based blends typically have significantly lower heats of combustion than No. 2 diesel. The aforementioned study by Goering *et al.* (19) reported heats of 37,045 kJ/kg for SBO/*n*-butanol/E95 and 36,687 kJ/kg for SBO/(*n*-butanol/triethylammonium linoleate)/E95 blends. Although these values were nearly 20% less than the heat of combustion (45,343 kJ/kg) of No. 2 diesel, short-term engine tests showed that co-solvent blends produced nearly as much power. Apparently, oxygenated components of the blends allowed leaner combustion yielding a 6% gain in thermal efficiency at full power.

SBO/**A**- and sunflowerseed oil/**A**-based blends were reported to pass the 200 h Engine Manufacturers' Association (EMA) durability screening test (20–22). Although the vegetable oil-fuels produced less bearing wear during testing, engine tear-downs revealed heavier carbon and lacquer deposits than for reference fuel. Though not as extensive, the deposits were similar to those noted from engine testing of neat vegetable oils (6). Thus, deposit formation was attributed to effects of incomplete combustion of the triacylglycerols. Given that these vegetable oil/**A**-based blends consisted of 50+ vol% vegetable oil and <15% alcohol, their values (8.3 mm^2/s for the SBO blend; 6.3 mm^2/s for the sunflowerseed oil blend) may not have been sufficiently reduced to prevent durability problems. Emphasizing this point, the results of subjecting a 1:1 (vol/vol) mixture of SBO/*n*-butanol/E95 and No. 2 diesel (ν = 4.0 mm^2/s) to the 200 h EMA test resulted in significantly reduced engine deposits (21,23).

Fuels formulated with vegetable oils reduce NO_x, hydrocarbons, particulate matter, carbon monoxide (CO), and polyaromatic hydrocarbons in exhaust emissions (24–30). Fuels formulated with water reduce NO_x, particulates, CO, and smoke emissions (25–27,31–35). Apparently, water acts as a heat sink to reduce the temperature of combustion, resulting in a decrease of NO_x and other harmful products in the exhaust. Alcohols such as methanol and ethanol can also reduce the temperature of combustion (33,35–37). Thus, evidence suggests combustion of vegetable oil/**A**/methanol (or ethanol) blends should yield similar reductions in harmful exhaust emissions. In contrast to the aforementioned effects of methyl esters on NO_x emissions, vegetable oil/**A**-based blends may have a distinct advantage as a clean burning fuel.

Vegetable oil/**A**-based blends may also have an economic edge over methyl esters. Transesterification usually requires catalyst (with periodic regeneration or replacement), heat (energy), and noncontinuous batch or semibatch processing. In contrast, formulating vegetable oil/**A**-based blends requires no catalyst, consumes very little energy, and adapts readily to continuous processing. In many cases, only slight agitation is necessary, and conversion time is negligible. Depending upon the surfactant costs, dilution of vegetable oil with relatively inexpensive methanol can greatly decrease fuel production costs relative to biodiesel.

The work reported herein examines one aspect of vegetable oil/**A**-based formulations that has received very little attention—low-temperature phase behavior and its impact on the application of these blends as alternative diesel fuels. Solutions were formulated from the following components: (i) oil = SBO or 2:1 (vol/vol) No. 2 diesel/SBO; (ii) **A** = 8:1 (mol) *n*-butanol/oleyl alcohol, 6:1 (mol) 2-octanol/triethylammonium linoleate, 4:1 (mol) 2-octanol/Unadol 40 (linoleyl alcohol), or *n*-butanol; and (iii) alcohol = methanol or E95. One blend (SBO/*n*-butanol/E95) was studied in 1:1 (vol/vol) mixtures with No. 2 diesel. Phase equilibria at 0 and 30°C were examined by comparing maximum alcohol solubility at constant **A**/oil mass ratio. Phase separation temperatures (T_φ) were determined as a function of **A**/oil mass ratio with respect to constant mass fraction of alcohol. Finally, CP data of blends were qualitatively compared with corresponding T_φ results.

EXPERIMENTAL PROCEDURES

Materials. Alkali-refined bleached SBO ($\rho^{25°C}$ = 0.912 g/mL) was from Archer Daniels Midland, Inc. (Decatur, IL). The fatty acid composition was 10.4% hexadecanoic, 4.2% octadecanoic, 25.4% 9*Z*-octadecenoic, 53.2% 9*Z*,12*Z*-octadecadienoic, and 6.8% 9*Z*,12*Z*,15*Z*-octadecatrienoic acids as confirmed by gas chromatographic analysis using a Varian (Sunnyvale, CA) 3400 GC with a Supelco (Bellefonte, PA) SP2380 column (30 m × 0.32 mm). Technical-grade oleyl alcohol (65% 9*Z*-octadecen-1-ol) and 2-octanol (98%) were from Aldrich (Milwaukee, WI). Unadol 40 (54% 9*Z*,12*Z*-octadecadien-1-ol), derived from SBO fatty acids, was from Sherex (New York, NY). Emersol 315 (59.0% 9*Z*,12*Z*-octadecenoic acid), derived from SBO, was from Emery Industries (Cincinnati, OH). Triethylamine (99+ %) and *n*-hexanol (99%) were from Sigma (St. Louis, MO). Analytical-grade methanol (99+ %) was from EM Science (Gibbstown, NJ); E95 was from Millennium Petrochemicals, Inc. (Iselin, NJ); and *n*-butanol (99.8%) was from Fisher Scientific (Pittsburgh, PA). Methanol, *n*-butanol, *n*-hexanol, and 2-octanol were stored over 4Å molecular sieves from Union Carbide (Danbury, CT) when not in use. Samples containing fatty acids,

fatty alcohols, or SBO were refrigerated at 0–5°C when not in use. Low-sulfur (<0.05 wt%) Phillips standard diesel fuel from the National Institute for Petroleum and Energy Research (Bartlesville, OK) was used in most of the studies reported in this work. Amoco standard diesel fuel provided by the University of Illinois (Urbana, IL) was used for some ν measurements.

Methods. The order of mixing of components was not critical. At room temperature (25°C), slight agitation of mixtures was necessary to produce single-phase translucent solutions. Triethylammonium linoleate formed spontaneously upon mixing of equimolar proportions of triethylamine and Emersol 315 in solution with SBO. Methanol and E95 solubility curves and T_{φ} data were determined by the method of phase volumes as described elsewhere (16). Studies near or above room temperature were conducted employing a Neslab (Portsmouth, NH) EX-410 constant temperature bath. Studies at subambient temperatures were conducted in a Neslab LT-50 refrigerated bath. Bath temperatures were constant to within 0.5°C. Apparatus for measuring CP was from Koehler (Bohemia, NY) and methods were in accordance with ASTM standards. Viscosity (ν) data were measured in accordance with ASTM standard methods using calibrated Cannon-Fenske viscometers from Cannon (State College, PA). Measurements at 40°C were conducted in a Cannon CT-1000 constant temperature bath while those at 0°C were conducted in a Cannon TE-1000 constant temperature bath. Both viscometer baths were accurate to within 0.1°C.

RESULTS AND DISCUSSION

In this work, the term "system" refers to an arbitrary mixture of oil [SBO or 2:1 (vol/vol) No. 2 diesel/SBO], **A** (one or two amphiphilic compounds), and a low-molecular weight alcohol (methanol or E95). Six of the seven systems represented in Table 1 were developed with **A** consisting of a long-chain surfactant (oleyl alcohol, Unadol 40, or triethylammonium linoleate) plus a medium-chain alkanol (*n*-butanol, *n*-hexanol

TABLE 1
Phase Separation of Selected Oil/Co-Solvent (A)/Low-Molecular Weight Alcohol Solutions[a]

System	Solution	Components[b]	Mass fraction	**A**/oil (g/g)	Type of separation[c]
1	**FS1**	SBO	0.400	0.902	I
		n-Butanol	0.250		
		Oleyl alcohol	0.111		
		Methanol	0.239		
2	**FS2**	SBO	0.307	1.218	I
		2-Octanol	0.246		
		Triethylammonium linoleate	0.128		
		Methanol	0.319		
2	**FS2a**	SBO	0.513	0.473	II
		2-Octanol	0.193		
		Triethylammonium linoleate	0.050		
		Methanol	0.244		
3	**FS3**	SBO	0.415	0.814	I
		2-Octanol	0.223		
		Unadol 40	0.115		
		Methanol	0.247		
5	**FS5**	No. 2 diesel fuel[d]	0.497	0.247	I
		SBO	0.267		
		n-Butanol	0.189		
		E95	0.047		
6	**FS6**	SBO	0.375	0.905	II
		n-Hexanol	0.260		
		Oleyl alcohol	0.079		
		Methanol	0.286		
7	**FS7**	SBO	0.415	0.814	II
		2-Octanol	0.223		
		Oleyl alcohol	0.115		
		Methanol	0.247		
8	**FS8**	SBO	0.375	0.905	II
		n-Hexanol	0.260		
		Unadol 40	0.079		
		Methanol	0.286		

[a]E95 = aqueous ethanol (95 vol%); SBO = soybean oil; Unadol 40 = fatty alcohols derived from SBO fatty acids.
[b]**System 1: A** = 8:1 (mol) *n*-butanol/oleyl alcohol; **System 2: A** = 6:1 (mol) 2-octanol/triethylammonium linoleate; **System 3: A** = 4:1 (mol) 2-octanol/Unadol 40; **System 5**: Oil = 2:1 (vol) No. 2 diesel fuel/SBO; **System 6: A** = 9:1 (mol) *n*-hexanol/oleyl alcohol; **System 7: A** = 4:1 (mol) 2-octanol/oleyl alcohol; **System 8: A** = 9:1 (mol) *n*-hexanol/Unadol 40.
[c]See Scheme 1 for details.
[d]Low sulfur (0.05 wt%) Phillips standard No. 2 diesel fuel.

or 2-octanol). The seventh system (**System 5**) had a single-component **A** (*n*-butanol). The notation **FS*n*** refers to a candidate alternative diesel fuel formulation derived from **System *n*** (***n*** = 1, 2, 3, 5, 6, 7, or 8). Mass fractions for oil, **A**, and alcohol (methanol or E95) for eight candidate formulated solutions are shown in Table 1 (**System 2** has two candidate formulations, **FS2** and **FS2a**).

Anisotropic phase behavior in SBO co-solvent blends. Scheme 1 shows two types of anisotropic phase behavior that may occur as the temperature of an unagitated blend decreases (left-to-right). For a Type I phase separation (Scheme 1A), crystallization of high melting point molecules causes the formation of solid crystals suspended in bulk liquid. As the ambient temperature T approaches T_φ (defined as the equilibrium temperature where phase separation is observed), the suspension of solid crystals resembles a cloudy phase. Thus, Type I phase separation exhibits "CP-like" behavior. For a Type II separation (Scheme 1B), the ability of **A** to solubilize an oil–alcohol mixture is neutralized, and the solution separates into two immiscible and translucent liquid layers. In this case, $T_\varphi \sim T_{critical}$ (critical solution temperature). As temperature decreases below T_φ, solutions exhibiting Type II behavior may undergo a second phase separation (at T_φ') where nucleation, crystal growth, and agglomeration predominate in the bottom (oil) layer. Under these circumstances, phase behavior in the oil layer resembles the crystallization characteristics of a low-alcohol content mixture of solvent (oil) and **A** components. For both Type I and II separations, decreasing temperatures further below T_φ causes formation of a solid or gel phase.

Results from qualitative analysis of the anisotropic phase behavior for the candidate fuel solutions are given in Table 1. As temperature decreased to T_φ, solutions **FS1**, **FS2**, **FS3**, and **FS5** underwent a transition from translucent liquid to a suspension of very small crystals in solution, resembling a Type I separation. In many cases, once transition from a cloud-like suspension into a solid–gel was underway (at $\mathbf{T} < T_\varphi$ in Scheme 1), a small layer of translucent liquid formed near the top of the mixture. This top layer was excess alcohol, formed as its relative solubility in the oil phase decreased with decreasing temperature.

In contrast, solutions **FS2a**, **FS6**, **FS7**, and **FS8** underwent a transition from one to two translucent liquid layers, resembling a Type II separation. Although **FS6**, **FS7**, and **FS8** each had T_φ ($T_{critical}$) values in the range –5 to 0°C, **FS2a** underwent phase separation at just below room temperature (25°C). It is possible the higher T_φ value for **FS2a** resulted from employing triethylammonium linoleate rather than an unsaturated fatty alcohol as surfactant in **A**. However, this conclusion is speculative, given the fatty amine and fatty alcohols studied in this work were technical grade.

A more likely (and less problematic) explanation has to do with **A**/oil mass ratio. For **FS2a**, **A**/oil = 0.473 g/g, a value that was significantly less than for **FS6**, **FS7**, and **FS8** (0.816–0.905 g/g). Increasing the **A**/oil mass ratio for **System 2** from 0.473 to 1.218 g/g (**FS2** in Table 1) decreased T_φ to coincide with the range (–5 to 0°C) noted earlier for **FS6**, **FS7**, and **FS8**. On the other hand, increasing **A**/oil mass ratio also changed the anisotropic phase behavior from Type II to Type

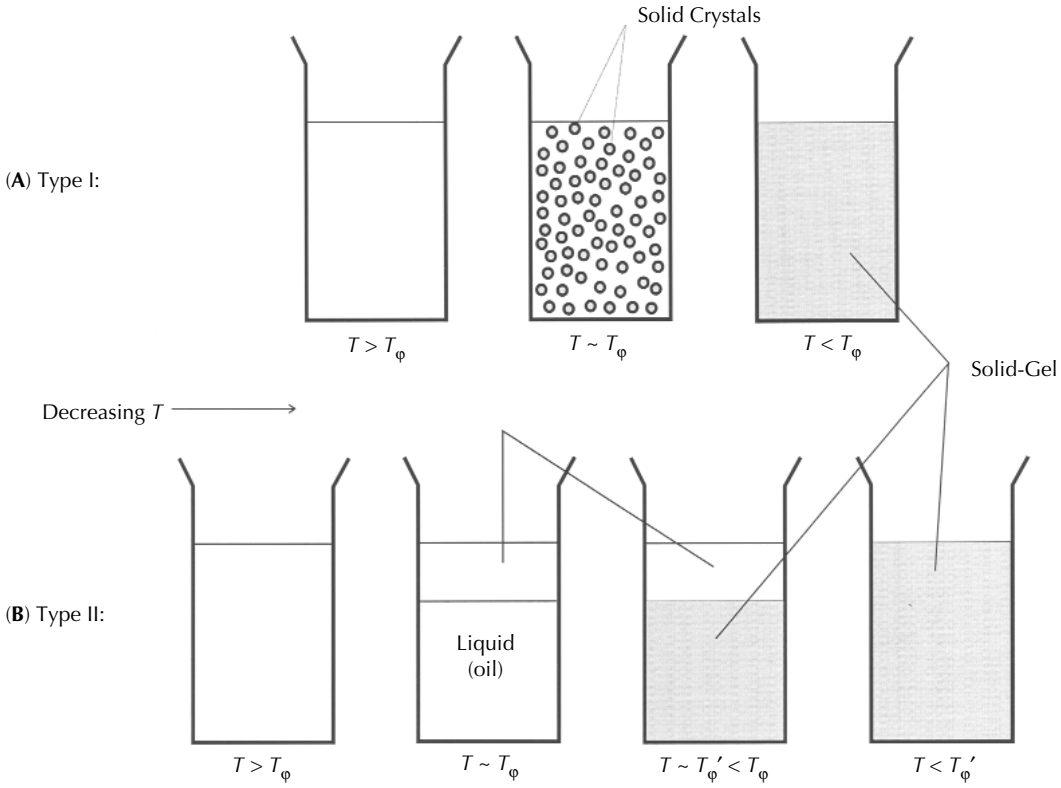

SCHEME 1

I separation. Effects of the **A**/oil mass ratio will be discussed shortly.

With respect to blends with fatty alcohols, anisotropic phase behavior may be affected by variances in surfactant tailgroup structure. Solution **FS3** [**A** = 4:1 (mol) 2-octanol/Unadol 40] was nearly identical to **FS7** [**A** = 4:1 (mol) 2-octanol/oleyl alcohol], with respect to mass fractions oil **A**, and methanol and with respect to T_φ values in the range –5 to 0°C. However, **FS3** showed Type I while **FS7** showed Type II separation. Unadol 40 has a higher CP (17°C) than oleyl alcohol (10°C). In general, an increasing degree of unsaturation decreases rather than increases the melting point of a long-chain fatty compound. The fatty alcohol surfactants used in this work were technical grade, leading to the conclusion that the 35 wt% fraction in oleyl alcohol that was not 9*Z*-octadecen-1-ol contained compounds that crystallize at higher temperatures than the 15–20 wt% total saturated fatty alcohol (primarily 1-hexadecanol and 1-octadecanol) fraction in Unadol 40. Nevertheless, reducing the apparent CP of the fatty alcohol surfactant appears to change the corresponding phase separation from Type I to Type II.

The structure of the medium chain-length alkanol constituent in **A** can also influence anisotropic phase behavior. Five solutions; **FS1**, **FS3**, **FS6**, **FS7**, and **FS8**—all had similar **A**/oil mass ratios (0.814 - 0.905) and gave similar results (T_φ = –5 to 0°C). Comparison of **FS1**, **FS6**, and **FS7** shows that increasing alkanol tailgroup chain length favors Type II separations. Similar comparison of **FS3** and **FS8** shows that increasing the degree of branching favors a Type I separation. It is known that increasing chain length or decreasing branching in an amphiphilic tailgroup increases solubilization of methanol in vegetable oil solutions (12,15). Apparently, increasing solubility of methanol by altering the alkanol constituent in **A** influences anisotropic phase behavior. The effects of medium chain-length alkanol tailgroup structure will be discussed shortly.

Effect of crystallization properties of oil on T_φ. Precise (±0.5°C) measurements of T_φ for solutions **FS1**, **FS2**, **FS3**, and **FS5** are listed in Table 2. These results show that **FS1**, **FS2**, and **FS3** had T_φ values that were only 1.5–5.5°C greater than T_φ of neat SBO. These solutions also exhibited anisotropic phase behavior similar to that of neat SBO. Solution **FS5**, which contained 0.497 mass fraction No. 2 diesel, gave the lowest T_φ, or –16°C, a value that was nearly identical to the CP of the neat diesel fuel (7). Not surprisingly, the relatively high quantity of diesel fuel in the formulation provided more efficient solubilization characteristics than neat SBO at cooler temperatures. These results demonstrate that the effects of low temperatures on the bulk oil phase dominate phase separation characteristics in vegetable oil/**A** blends.

Effect of ***A****/oil mass ratio on alcohol solubility.* Figure 1 is a comparison of alcohol solubility where x_{alc} = mass fraction of alcohol (methanol or E95) in **Systems 1** and **5** at 0 and 30°C. In this figure, anisotropic phase separation occurred as the mass fraction of alcohol increased across the solubility curve. In addition, phase separations at 0°C were typically Type I while those at 30°C were Type II. **Systems 2** and **3** (not graphically presented) exhibited analogous behavior with respect to type of phase separation at 0 and 30°C.

TABLE 2
Comparison of Phase Separation Temperature (Tj) and Low-Temperature Properties of SBO-Derived Co-solvent Blends and Biodiesel Formulations[a]

Formulation	T_φ (°C)	CP (°C)	ν @ 40°C (mm^2/s)	ν @ 0°C (mm^2/s)
FS1	–0.5	5	3.55	14.0
FS2	1.5	5	3.90	16.1
FS3	–3.5	–8	5.12	16.8
FS5	–16	–16	4.13	14.3
SBO	–4	–6	32.8	188
2:1 (vol) No. 2 diesel/SBO[e]	—	–18[b]	6.49[b]	24.6[b]
Methyl soyate	—	0	4.34	11.4[c]
"B20"	—	–14	2.99	11.6[d]
"B30"	—	–10	3.18	12.0[d]
No. 2 diesel fuel[e]	—	–16	2.81	10.4[d]

[a]ν = kinematic viscosity; CP = cloud point; "B20" = 4:1 (vol) No. 2 diesel/methyl soyate blend; "B30" = 7:3 (vol) No. 2 diesel:methyl soyate blend. See Table 1 for other definitions and abbreviations.
[b]Amoco standard diesel fuel.
[c]At +5°C.
[d]At –3°C.
[e]Data for No. 2 diesel fuel, methyl soyate and No. 2 diesel/methyl soyate blends are from Reference 7.

At 30°C, an increasing mass fraction of alcohol eventually caused phase separation into two translucent, immiscible liquid layers. The top layer was primarily low-molecular weight alcohol whereas the bottom layer was predominantly oil (SBO or diesel fuel/SBO). These solubility curves were dissimilar with respect to variations in solubility limits for alcohol (methanol or E95) in their respective **A**/oil mixtures.

On the other hand, at 0°C curves for **Systems 1** and **5** were nearly coincidental (±0.01 mass fraction alcohol). Crystalliza-

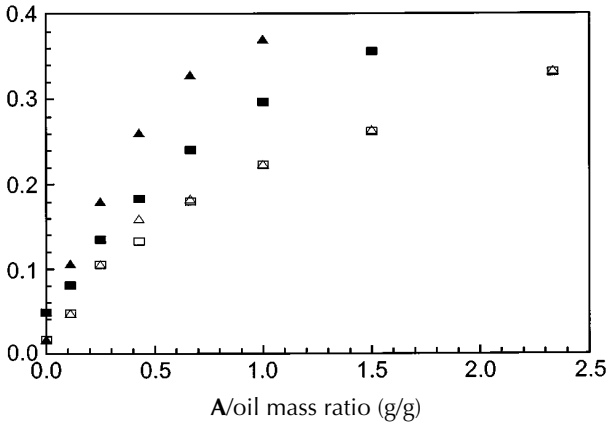

FIG. 1. Effect of **A**/oil mass ratio on alcohol solubility. ❑, **System 1** at 0°C; ■, **System 1** at 30°C; △, **System 5** at 0°C; ▲, **System 5** at 30°C; x_{alc}, mass fraction of alcohol (methanol for **System 1**, E95 for **System 5**). **System 1**, Components (mass fraction): soybean oil (SBO: 0.400); *n*-butanol (0.250); oleylalcohol (0.111); methanol (0.239). **System 5**: No. 2 diesel fuel (0.497); SBO (0.267); *n*-butanol (0.189); 95 wt% ethanol (E95: 0.047). **A**, co-solvent (consisting of amphiphilic compound plus surfactant. Oil, SBO for **System 1**; 2:1 (vol) No. 2 diesel/SBO for **System 5**.

tion of high-melting compounds present in **A** (from oleyl alcohol) in **System 1** and in SBO in both systems becomes more of a factor in mechanisms driving phase separation at lower temperatures. Thus, the effectiveness of oleyl alcohol decreases, leaving *n*-butanol as the predominating solubilizing component in **A** for **System 1**. As a result, the active **A**-component for both **Systems 1** and **5** becomes *n*-butanol, resulting in nearly identical alcohol solubility curves in Figure 1.

A similar comparison (not graphically presented) of methanol solubility curves for **Systems 2** and **3** gave nearly coincident curves at 30°C (±0.025 mass fraction methanol) and somewhat coincident curves at 0°C (±0.05 mass fraction). Given that **A**-constituents varied with respect to surfactant (fatty amine for **System 2**; fatty alcohol for **System 3**), these results indicate that such variations may not significantly affect anisotropic phase behavior as suggested earlier in this work. Again, this conclusion is speculative given the technical grade of the surfactants studied.

Nevertheless, results in Figure 1 indicate that anisotropic phase behavior of a given vegetable oil/**A**-based blend will be influenced by the presence of high melting point compounds in its solvent (oil) and **A** constituents. That is, if T_φ occurs at a temperature sufficient to avert crystallization in solvent or **A** components (for example, if T_φ exceeds room temperature), then a Type II separation is favored. Otherwise, if $T_{critical}$ is less than T_φ, then a Type I separation is favored.

Results for solutions **FS2** and **FS2a** (Tables 1 and 2) support this hypothesis. It was noted earlier in this work that increasing **A**/oil mass ratio from 0.473 (**FS2a**) to 1.218 g/g (**FS2**) significantly decreased T_φ. This decrease coincided with a change from Type II to Type I phase separation. In other words, although the mass fraction of methanol increased by nearly 25%, T_φ decreased. Thus, the influence of methanol on anisotropic phase behavior diminished between **FS2a** and **FS2**. Increasing **A**/oil mass ratio increased the solubility of methanol in **System 2** at lower temperatures. As a result, anisotropic behavior in **FS2** becomes dominated by the crystallization characteristics of compounds present in SBO and **A** (triethylammonium linoleate).

Effect of A/oil mass ratio on T_φ. The effects of increasing **A**/oil mass ratio on T_φ are shown in Figures 2 and 3. Figure 2 is a plot of results for **Systems 1**, **2**, **3**, and **5** with methanol and E95 mass fractions = 0.000; Figure 3 is a plot of results for **Systems 1**, **2**, and **3** with methanol mass fraction = 0.200. These results show that adding methanol to **Systems 1–3** significantly increased T_φ, particularly at lower **A**/oil mass ratios. Thus, the presence of low-molecular weight alcohol influences anisotropic phase behavior in vegetable oil/**A** mixtures, with respect to constant **A**/oil mass ratio.

In Figure 2, anisotropic phase behavior in **Systems 1**, **2**, **3**, and **5** was governed by interactions between constituent solvent and **A** molecules present in solution. Curves for **Systems 1**, **2**, and **3** were nearly coincident (±1.0°C), indicating similar phase separation mechanisms in these systems. **Systems 1**, **2**, and **3** gave T_φ values in the range –11 to –6°C, while

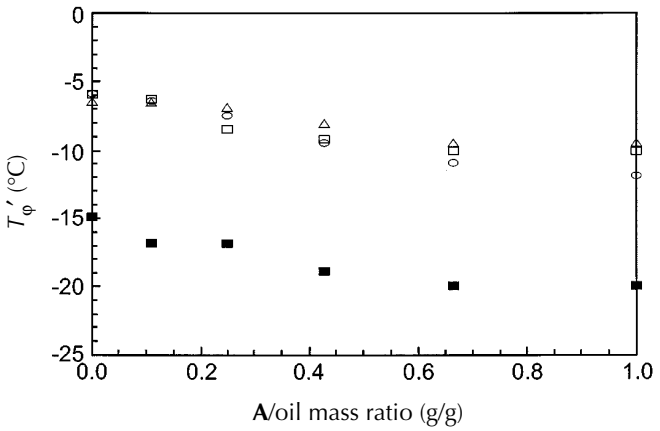

FIG. 2. Phase equilibria with respect to mass fraction of methanol = 0.000 g/g. ❑, **System 1**; △, **System 2**; ○, **System 3**; ▲, **System 5**. **System 1**, Components (mass fraction): SBO (0.307); 2-octanol (0.246); triethylammonium linoleate (0.128); methanol (0.319). **System 3**: SBO (0.415); 2-octanol (0.223); Unadol (0.115); methanol (0.247). Oil, SBO for Systems 2 and 3. See Figure 1 for other definitions and abbreviations.

System 5 gave T_φ values in the range –20 to –15°C. Thus, the four curves were in a temperature range sufficiently low to allow crystallization of high melting point constituent solvent and **A** molecules. As a result, all four systems exhibited Type I separations for **A**/oil mass ratios in the range 0.000–1.000.

In contrast, results in Figure 3 indicate that adding methanol to **Systems 1**, **2**, and **3** alters the interactions between constituent solvent and **A** molecules, leading to an increase in T_φ. The hypothesis presented in the preceding section stated that elevation of T_φ to a range sufficient to prevent nucleation and crystallization of constituent solvent or **A** molecules in solution favors a Type II separation. In reality, under most conditions, systems in Figure 3 showed formation of a slightly turbid suspension of very small particles as temperatures approached T_φ. For solutions with $T_\varphi \geq 25$°C, the particles resembled very small liquid methanol droplets that formed prior to coalescence into a separate liquid layer. For solutions with relatively low T_φ values (< –5°C), the particles

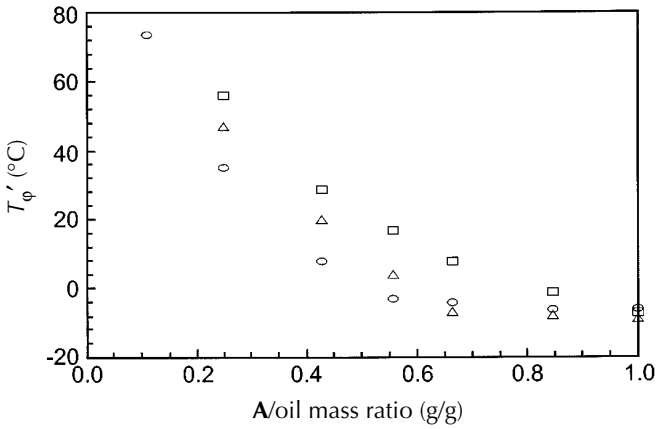

FIG. 3. Phase equilibria with respect to mass fraction of methanol = 0.200 g/g. Legend: ❑, **System 1**; △, **System 2**; ○, **System 3**. See Figures 1 and 2 for other definitions and abbreviations.

were solid crystals from a Type I separation, resembling anisotropic behavior described above for Figure 2. Finally, for solutions with intermediate T_φ values (–5°C– upper melting temperature of solid crystals), the particles were likely a mixture of both small liquid droplets and crystals suspended in solution.

Results in Figures 2 and 3 show that increasing **A**/oil mass ratio generally decreases T_φ. Curves in Figure 2 decreased slightly (~5°C) as the mass ratio increased from 0.000 to 1.000 g/g, where as corresponding curves in Figure 3 showed similar behavior only at relatively high mass ratios. At **A**/oil > 0.700 g/g (Fig. 3), T_φ curves for **Systems 2** and **3** converged at T_φ values in the range –8 to –5°C and became nearly independent of **A**/oil mass ratio. Furthermore, at **A**/oil ~ 1 g/g, the curve for **System 1** appears to converge with the other two systems. Finally, the temperature range where curves converged in Figure 3 was similar to that for systems at zero-alcohol content in Figure 2. These results suggest that mechanisms for nucleation and crystalline growth in solutions whose T_φ are nearly independent of **A**/oil mass ratio are not greatly affected by the presence of methanol, up to a mass fraction of methanol = 0.20.

Analogous to results shown in Figure 2, solutions whose T_φ were nearly independent of **A**/oil mass ratio in Figure 3 underwent Type I separations. Thus, increasing **A**/oil mass ratio favors Type I separations. Although decreasing the mass ratio in the high-T_φ range promoted Type II separations, it was already noted that the systems in Figure 3 generally exhibited formation of small liquid droplets under these conditions. Only solutions with very low **A**/oil mass ratios demonstrated outright Type II separation. For example, **Systems 2** and **3** separated into two liquid layers when **A**/oil ≤ 0.100 and $T_\varphi \geq 47$°C for **System 2**, or ≥70°C for **System 3**.

Analogous results (not graphically presented) for systems with mass fractions of methanol of 0.25, 0.30, and 0.35 showed that the minimum **A**/oil mass ratio where T_φ curves converge to and become nearly independent of mass ratio increases with mass fraction of methanol. In addition, increasing the mass fraction of methanol increased the **A**/oil mass ratio limit for Type II separations. For example, **System 1** exhibited Type II separation at **A**/oil ≤ 0.250 g/g for a 0.250 mass fraction of methanol, at **A**/oil ≤ 0.430 for a 0.300 mass fraction of methanol, and at **A**/oil ≤ 0.550 for mass fraction of methanol = 0.35.

Low-temperature flow properties of co-solvent blends. Listed in Table 2 are CP and ν (at 40 and 0°C) data for four formulated solutions, neat oils (SBO, No. 2 diesel, and 2:1 (vol/vol) diesel/SBO), plus methyl soyate and two diesel fuel/methyl soyate blends.

Although **FS1** and **FS2** had higher CP, **FS3** had a significantly lower CP than methyl soyate. Solution **FS5** had a CP less than that of "B20" (20 vol% methyl soyate blend) and nearly equivalent to that of neat diesel fuel. Comparison of T_φ results also indicates that **FS3** and **FS5** performed better than **FS1** and **FS2**. Solutions **FS1** and **FS2** each gave CP that were 3.5–5.5°C higher than their corresponding T_φ values. This was likely caused by variances in experimental conditions applied to measurement of CP and T_φ. In general, CP is determined under non-steady state conditions where the rate of heat loss varies during measurement. In contrast, T_φ is measured under near-steady state (equilibrium) conditions.

The four SBO/**A**-based blends gave ν results that were comparable with methyl soyate blends at 40°C and slightly higher at 0°C. Solutions **FS1**, **FS2**, and **FS5** gave lower ν values than neat methyl soyate at 40°C. Although these solutions gave higher ν values at 0°C, the increase in ν is less than 5.0 mm^2/s, an increase that was reasonable given the data for methyl soyate in Table 2 were actually measured at +5°C to prevent formation of solids during equilibration (7). Aside from neat SBO, the diesel fuel/SBO mixture and **FS3** gave the highest values at both 40 and 0°C. **FS5** also has a comparable ν value at 40°C and only a slightly larger ν value at 0°C than B20 (measured at –3°C).

Overall, these results show that SBO co-solvent blends may be formulated to give comparable to superior low-temperature flow performance with respect to fatty acid methyl esters. Like methyl esters, co-solvent blends may themselves be blended with No. 2 diesel to give improved low-temperature performance.

Anisotropic phase behavior will dictate the nature of operability problems that may occur when alternative diesel fuels formulated from vegetable oil/**A**-based blends are subjected to decreasing temperatures. For Type I separations, crystals continue to grow and agglomerate as temperatures decrease or remain constant below T_φ. When crystals become large enough (~10 μm) they will restrict flow through fuel lines and block filters, eventuating in fuel starvation and stalled engines. For Type II separations at or below T_φ, separation into two layers can cause a number of operability and performance problems associated with combustion of neat alcohols (including ignition delay and decrease in power output) or vegetable oils (substantially increased viscosities and incomplete combustion). Hence, characterization of candidate vegetable oil/**A**-based blends with respect to fuel properties cannot overlook anisotropic phase behavior at lower temperatures during fuel formulation.

Regardless of the nature of anisotropic phase behavior, the work reported herein may be employed to demonstrate several practical methods for maintaining isotropic phase behavior of SBO/**A**-based blends at low-temperatures. The most flexible method is to alter constituents in **A**. Replacing the long-chain fatty alcohol or amine with more compatible surfactants may significantly reduce the temperature where nucleation initiates. Increasing the tailgroup length of the medium-chain alkanol improves solubilization of methanol or E95 at low temperatures. Increasing **A**/oil mass ratio also increases methanol or E95 solubility at low temperatures. Although this method can significantly reduce T_φ, results indicate that T_φ is nearly independent of **A**/oil mass ratio at relatively high mass ratios. Mixing blends with petroleum middle distillates also promotes isotropic phase behavior at lower temperatures. This method has the added advantage of mak-

ing the fuel less costly. A less practical method for decreasing T_φ would be to reduce the low molecular weight alcohol content of the blend. This method may have the disadvantage of increasing ν, an effect that may lead to engine deposits and other durability problems associated with incomplete combustion.

ACKNOWLEDGMENTS

Dale Ehmke, Haita Khoury and Rebecca (Burke) Zick provided technical assistance for experimental studies and analyses.

REFERENCES

1. Goering, C.E., M.D. Schrock, K.R. Kaufman, M.A. Hanna, F.D. Harris, and S.J. Marley, Evaluation of Vegetable Oil Fuels in Engines, in *Proceedings of the 1987 International Winter Meeting of the ASAE*, American Society of Agricultural Engineers, St. Joseph, 1987, Paper No. 87-1586.
2. Schwab, A.W., M.O. Bagby, and B. Freedman, Preparation and Properties of Diesel Fuels from Vegetable Oils, *Fuel 66*: 1372–1378 (1987).
3. Ziejewski, M., H. Goettler, and G.L. Pratt, Comparative Analysis of the Long-Term Performance on a Diesel Engine on Vegetable Oil Based Alternate Fuels, in *SAE Tech. Paper Ser.*, Society of Automotive Engineers, Warrendale, 1986, Paper No. 860301.
4. Ziejewski, M., H. Goettler, and G.L. Pratt, Influence of Vegetable Oil Based Alternate Fuels on Residue Deposits and Components Wear in a Diesel Engine, in *SAE Tech. Paper Ser.*, Society of Automotive Engineers, Warrendale, 1986, Paper No. 860302.
5. Engler, C.R., and L.A. Johnson, Effects of Processing and Chemical Characteristics of Plant Oils on Performance of an Indirect-Injection Diesel Engine, *J. Am. Oil Chem. Soc. 60*: 1592–1596 (1983).
6. Ryan, T.W., III, L.G. Dodge, and T.J. Callahan, The Effects of Vegetable Oil Properties on Injection and Combustion in Two Different Diesel Engines, *Ibid. 61*:1610–1619 (1984).
7. Dunn, R.O., and M.O. Bagby, Low-Temperature Properties of Triglyceride-Based Diesel Fuels: Transesterified Methyl Esters and Petroleum Middle Distillate/Ester Blends, *Ibid. 72*:895–904 (1995).
8. Knothe, G., R.O. Dunn, and M.O. Bagby, Biodiesel: The Use of Vegetable Oils and Their Derivatives as Alternative Diesel Fuels, in *Fuels and Chemicals from Biomass*, ACS Symp. Ser. No. 666, American Chemical Society, Washington, DC, 1997, pp. 172–208.
9. Chang, D.Y.Z., J.H. Van Gerpen, I. Lee, L.A. Johnson, E.G. Hammond, and S.J. Marley, Fuel Properties and Emissions of Soybean Oil Esters as Diesel Fuel, *J. Am. Oil Chem. Soc. 73*: 1549–1555 (1996).
10. Krahl, J., A. Munack, M. Bahadir, L. Schumacher, and N. Elser, Survey About Biodiesel Exhaust Emissions and Their Environmental Effects, in *Proceedings of the Third Liquid Fuel Conference: Liquid Fuel and Industrial Products from Renewable Resources*, American Society of Agricultural Engineers, St. Joseph, 1996, pp. 136–148.
11. Ali, Y., and M.A. Hanna, Alternative Diesel Fuels from Vegetable Oils, *Bioresource Technol. 50*:153–163 (1994).
12. Dunn, R.O., and M.O. Bagby, Solubilization of Methanol and Triglycerides: Unsaturated Long-Chain Fatty Alcohol/Medium-Chain Alkanol Mixed Amphiphilic Systems, *J. Am. Oil Chem. Soc. 71*:101–108 (1994).
13. Dunn, R.O., A.W. Schwab, and M.O. Bagby, Solubilization and Related Phenomena in Nonaqueous Triolein/Unsaturated Long Chain Fatty Alcohol/Methanol Solutions, *J. Dispersion Sci. Technol. 14*:1–16 (1993).
14. Schwab, A.W., H.C. Nielsen, D.D. Brooks, and E.H. Pryde, Triglyceride/Aqueous Ethanol/1-Butanol Microemulsions, *Ibid. 4*:1–17 (1983).
15. Schwab, A.W., and E.H. Pryde, Triglyceride–Methanol Microemulsions, *Ibid. 6*:563-574 (1985).
16. Dunn, R.O., A.W. Schwab, and M.O. Bagby, Physical Property and Phase Studies of Nonaqueous Triglyceride/Unsaturated Long Chain Fatty Alcohol/Methanol Systems, *Ibid. 13*:77–93 (1992).
17. Dunn, R.O., G. Knothe, and M.O. Bagby, Recent Advances in the Development of Alternative Diesel Fuel from Vegetable Oils and Animal Fats, in *Recent Res. Develop. Oil Chem. 1*:31–56 (1997).
18. *ASTM D975: Standard Specification for Diesel Fuel Oi*ls, American Society for Testing and Materials, West Conshohocken, 1995.
19. Goering, C.E., A.W. Schwab, R.M. Campion, and E.H. Pryde, Soyoil-Ethanol Microemulsions as Diesel Fuel, *Trans. ASAE 26*:1602–1607 (1983).
20. Schwab, A.W., and E.H. Pryde, Microemulsions from Vegetable Oil and Lower Alcohol with Octanol Surfactant as Alternative Fuel for Diesel Engines, U.S. Patent. No. 4,557,734 (1985).
21. Goering, C.E., in Final Report for Project on Effect of Nonpetroleum Fuels on Durability of Direct-Injection Diesel Engines under Contract 59-2171-1-6-057-0, U.S. Department of Agriculture, Agricultural Research Service, Peoria, 1984.
22. Ziejewski, M., K.R. Kaufman, A.W. Schwab, and E.H. Pryde, Diesel Engine Evaluation of a Nonionic Sunflower Oil-Aqueous Ethanol Microemulsion, *J. Am. Oil Chem. Soc. 61*:1620–1626 (1984).
23. Goering, C.E., and B. Fry, Engine Durability Screening Test of a Diesel Oil/Soy Oil/Alcohol Microemulsion, *Ibid. 61*:1627–1632 (1984).
24. Murayama, T., Evaluating Vegetable Oils as a Diesel Fuel, *inform 5*:1138–1145 (1994).
25. Crookes, R.J., F. Kiannejad, and M.A. A. Nazha, Performance and Emissions of a 2.5 Litre Multi-Cylinder Direct-Injection Automotive Diesel Engine with Alternative Diesel Fuels and Emulsions, *Proceeding of the IMechE Seminar (Iss. 2) on Fuels for Automotive and Industrial Diesel Engines,* Institute of Eng. Mechanical Engineers, London, 1993, pp. 151–159.
26. Crookes, R.J., F. Kiannejad, G. Sivalingam, and M.A.A. Nazha, Effects of Using Vegetable Oil Fuels and Their Emulsions on the Performance and Emissions of Single- and Multi-Cylinder Diesel Engines, *Arch. Combust. 13*:57–74 (1993).
27. Crookes, R.J., M.A.A. Nazha, and F. Kiannejad, Single and Multi Cylinder Diesel-Engine Tests with Vegetable Oil Emulsions, in *SAE Tech. Paper Ser.*, Society of Automotive Engineers, Warrendale, 1992, Paper No. 922230.
28. Ziejewski, M., and H.J. Goettler, Comparative Analysis of the Exhaust Emissions for Vegetable Oil Based Alternative Fuels, in *SAE Spec. Publ. SP-900: Alternative Fuels for CI and SI Engines*, Society of Automotive Engineers, Warrendale, 1992. pp. 65-73, Paper No. 920195.
29. Ziejewski, M., H.J. Goettler, L.W. Cook, and J. Flicker, Polycyclic Aromatic Hydrocarbon Emissions from Plant Oil Based Alternative Fuels, in *SAE Tech. Paper Ser.*, Society of Automotive Engineers, Warrendale, 1991, Paper No. 911765.
30. Mills, G.A., and A.G. Howard, A Preliminary Investigation of Polynuclear Aromatic Hydrocarbon Emissions from a Diesel Engine Operating on Vegetable Oil-Based Alternative Fuels, *J. Inst. Energy 56*:131–137 (1983).
31. Crookes, R.J., F. Kiannejad, and M.A.A. Nazha, Systematic Assessment of Combustion Characteristics of Biofuels and Emul-

sions with Water for Use as Diesel Engine Fuels, *Energy Convers. Mgmt. 38*:1785–1795 (1997).
32. Lee, P.K., B.F. Szuhaj, and A. Diego, Evaluation of Soy Based Heavy Fuel Oil Emulsifiers for Energy Efficiency and Environmental Improvement, in *Proceedings, Bioenergy 96—The Seventh National Bioenergy Conference*, U.S. Department of Energy, Washington, DC, 1996, Vol. 1., pp. 372–376.
33. Kesling, H.S., Jr., F.J. Liotta, and J.M. McFarland, Oxygenated Microemulsion Diesel Fuel, *ACS Fuel Chem. Div. Preprints 39*:322–326 (1994).
34. Sexton, M.D., A.K. Smith, J. Bock, M.L. Robbins, S.J. Pace, and P.G. Grimes, Microemulsion Diesel Fuel Compositions and Method of Use, Eur. Patent No. EP 0 475 620 A2 (1992).
35. Schon, S.G., and E.A. Hazbun, Methanol as Cosurfactant for Microemulsions, U.S. Patent No. 5,004,479 (1991).
36. Schwab, A.W., and E.H. Pryde, Diesel Fuel-Aqueous Ethanol Microemulsions, U.S. Patent No. 4,451,265 (1984).
37. Boruff, P.A., A.W. Schwab, C.E. Goering, and E.H. Pryde, Evaluation of Diesel Fuel–Ethanol Microemulsions, *Trans. ASAE 25*:47–53 (1982).

[Received June 1, 1999; accepted August 31, 2000]